

UDC 621.315.592

XVII Interstate Conference „Thermoelectrics and Their Applications — 2021“  
(ISCTA 2021 St. Petersburg, September 13–16, 2021)

## Obtaining and investigation of ohmic contacts with high adhesion to thermoelements

© M.Yu. Shtern, A.O. Kozlov, Yu.I. Shtern, M.S. Rogachev<sup>✉</sup>, E.P. Korchagin, B.R. Mustafoev, A.A. Dedkova

National Research University of Electronic Technology,  
124498 Moscow, Zelenograd, Russia

<sup>✉</sup> E-mail: m.s.rogachev88@gmail.com

Received August 12, 2021

Revised August 28, 2021

Accepted August 28, 2021

The factors determining the adhesive strength of film coatings are considered. The functions of contacts in thermoelements used in a wide temperature range were determined. It was established that the adhesive strength of contact is a limiting factor in the mechanical strength of a thermoelement. A method of vacuum sputtering of thin-film contacts was proposed, including the surface treatment of samples of thermoelectric materials. The presence of a transition layer in the area of the metal–thermoelectric material contact, formed during the interaction of the metal with elements of the thermoelectric material, was established. The dependence of the adhesive strength of film contact on roughness of surface on which they formed was established. Thermal stable contacts for thermoelements with low resistivity of the order of  $10^{-9} \Omega \cdot \text{m}^2$  and high adhesion strength of at least 12 MPa were obtained by ion-plasma sputtering.

**Keywords:** thermoelements, contacts, thin films, adhesion, contact resistance.

DOI: 10.21883/SC.2022.14.53846.01

### 1. Introduction

In thermoelectric (TE) devices operating on the Peltier and Seebeck effects, the efficiency of thermoelements is largely determined by the quality of contacts, the purpose of which is to commutate the legs in thermoelements by means of junctions [1–5]. In addition, in thermoelements with multisection legs, the sections are commutated using contacts. It is advisable to use multisection legs in thermoelements with a wide range of operating temperatures [6–11]. In such a thermoelement, each section of leg operates in certain temperature range and is made of various thermoelectric materials having the maximum thermoelectric figure of merit at these temperatures.

The contacts should carry out reliable commutation, ensuring minimum heat and electrical losses. In thermoelements, the contacts perform the following functions: carry out an ohmic contact to the TE materials; are a barrier preventing mutual diffusion of the connected materials; provide high adhesive strength of contact systems to TE materials and between layers in the contact system. In simple thermoelements operating at low temperatures, contacts are usually made of one or two contact layers of metals, for example Ni or Ni/Au. In multisection thermoelements operating at wide temperature range, it is necessary to create contact multilayer systems [11–14], for example Ni/(Ta–W–N)/Ni or Mo/(Ta–W–N)/Ni [6].

There are several methods for the formation of contact layers in thermoelements. It is promising to obtain them by the method of vacuum sputtering [6,11,15–19], which provides a minimum value of contact resistance and good adhesive strength. In addition, vacuum sputtering can be used in combination with other methods, for example, chemical or electrochemical deposition of contact metal layers.

Thermoelectric devices and, accordingly, thermoelements operate at high temperature gradients, and generator thermoelements also operate at high temperatures up to 1200 K, often under conditions of increased vibration. Moreover, the construction of the thermoelement uses materials with different thermal expansion coefficients. All this leads to the appearance of significant mechanical stresses in the structure of the thermoelement. In this regard, it should be noted about the importance of studying the adhesive strength of contacts, which is a limiting factor in the mechanical strength of the thermoelement as a whole. The present work is dedicated to these studies.

### 2. Factors determining the adhesive strength of film coatings

Adhesion is always the result of intermolecular interaction of contacting bodies. The adhesive bond is due to either

covalent or ionic bonds or van der Waals forces. The chemical bond energy per molecule is greater than the energy of van der Waals forces. Therefore, other things being equal, the most significant adhesion occurs when a chemical reaction takes place on the interaction of bodies on their surfaces. As a rule, a chemical reaction leads to the appearance of an electric double layer formed by a system of dipoles oriented perpendicular to the contact surface [20].

The state of the surface of the base (substrate) is a decisive factor for adhesion of film [6,16,21–26]. Knowledge of the properties of a clean surface is a necessary starting point in understanding surface phenomena and is the basis for any discussion of the mechanisms of binding of foreign substances [21,23]. It should be noted that surface states arise as a result of the termination of the periodic structure (Tamm surface states) or as a result of the presence of a large number of impurity centers on the surface [23]. Therefore, preliminary cleaning of the substrate surface and its control determine good adhesion of films [6,21,27–29]. There are three types of surface irregularities that must be eliminated in order to be considered clean. The first is a foreign phase such as a metal oxide. The second is adsorbed gases and impurities. The third is structure disturbance of crystal lattice. The process of cleaning the surface from adsorbed gases and impurities, which is most common in thin-film technology, consists in breaking the bonds between impurity molecules and between the molecules of this impurity and the substrate. This can be achieved both by chemical means, such as solvent purification, or by applying sufficient energy to vaporize the impurity, such as by ion bombardment or heating. For porous substrates, the most effective degassing method is vacuum heat treatment. The term degassing refers to the processes of gas removal by desorption and diffusion [23]. The rates of desorption of impurities exponentially depend on temperature and therefore sharply increase when the substrate is heated. Low pressure in the chamber of the order of ( $10^{-6}$ – $10^{-8}$ ) Torr also significantly contributes to the degassing of substrates.

The amount of adhesion cannot be accurately calculated. In support of this fact, a number of relevant examples are given in [22]. Currently, there is no available, suitable for calculations and, most importantly, reliable method for the theoretical determination of the adhesion of specific materials in real conditions. Therefore, to assess adhesion in film technology, experimental studies of adhesion strength are required. It is necessary to distinguish between the concepts of equilibrium (true) adhesion, which occurs when solids are in contact, and adhesive strength, which is measured as a result of separation of films. Adhesive strength qualitatively characterizes true adhesion. In practice, it is possible to use various methods for the experimental determination of adhesive strength. However, the method of uniform normal tear of film allows the most accurate determination of the adhesive strength. In this case, it is expressed by the tear force per unit surface. At the same time distinguish the adhesion separation along the film-substrate interface and

cohesive separation, when destruction occurs along the film or substrate with the formation of a film-film, substrate-substrate interface. Mixed adhesive-cohesive separation of films is also possible [22].

In the formed films, internal mechanical stresses arise: intrinsic ones caused by the structure of the film and thermal ones, associated with the difference in the thermal linear expansion coefficients of the film and the substrate. Internal stresses reduce the adhesive strength and depend, among other things, on the surface roughness and film thickness [22,28]. Moreover, the magnitude of internal stresses can be of the same order of magnitude as the adhesive strength. This is observed, for example, in the vacuum formation of films of increased thickness. The technology for producing films has a significant influence on internal stresses. With the help of technological modes, it is possible to minimize the stresses in the film and thereby provide an increase in adhesive strength.

Taking into account the considered factors affecting the value of adhesion strength, it can be estimated by means of the force of separation of the film from the substrate as follows [22]:

$$F = F_a + F_g + F_e + F_n - F_{in}, \quad (1)$$

where  $F$  is the film tearing force,  $F_a$  is the adhesion force (equilibrium),  $F_g$  is the force applied to the deformation of the film,  $F_e$  is the force applied to overcome the emerging electrostatic interaction in the electric double layer,  $F_n$  is the force applied to overcome the mechanical roughness of the contacting surfaces,  $F_{in}$  is the force due to internal stresses in the film.

As a result, the force applied on adhesive tearing of the film is not equal to the force characterizing equilibrium adhesion. In most cases, the condition is realized when  $F > F_a$ , i.e. adhesion strength is generally greater than equilibrium adhesion. Thus, in the practical application of film coatings, in our case of contacts, it is the  $F$  value that determines the adhesive strength.

As noted above, the adhesion of the film to the substrate increases noticeably if the formation of chemical bonds between the film and the substrate occurs at the initial stage of deposition. When choosing the material of the contact layer, it is also necessary to take into account the possibility of mutual diffusion of the contacting materials. This can be accompanied by the formation of solid solutions or intermetallic compounds at contact interface, which have a lower value of electrical conductivity and mechanical strength. Therefore, in a number of cases, it is necessary to organize a diffusion barrier between the substrate and the deposited contact layer [6,11,13,14,30–32].

Summarizing the above, it should be noted that studies of the influence of various factors on the adhesive strength of the formed films is a necessary condition in the development of the technology of reliable contacts in thermoelements.

### 3. Experimental

#### 3.1. Preparation of samples of TE materials

As noted above, the state of the surface of TE materials, on which the contact layers are deposited, is a decisive factor for their adhesion, and also has a significant influence on the contact resistance. When obtaining and studying the contacts, we used  $\text{Bi}_{0.5}\text{Sb}_{1.5}\text{Te}_3$  samples obtained by extrusion.

At the initial stage, the surface of the samples of TE materials was subjected to mechanical treatment. The purpose of this operation is to remove the layer of TE materials damaged during cutting of the samples and to obtain the necessary surface roughness, which plays an important role in the adhesion strength of the deposited film. Mechanical treatment of TE materials is not an easy task, since the majority of thermoelectric materials are soft, with a microhardness of 25 to 70 kg/mm<sup>2</sup> [21,33–40]. This greatly complicates the grinding and polishing of TE materials. The technology of mechanical treatment of the surface of TE materials is presented by us in [21].

To study the dependence of the adhesion strength on the surface relief on which the Ni film was deposited, samples of TE material with various degrees of surface roughness were prepared. When forming contact systems in thermoelements, as a rule, the adhesive strength and transient contact resistance are determined by the contact layer formed directly on the surface of TE material. This is confirmed by a number of, including our works [6,11,12]. Ni has proven itself well as a contact material up to temperatures of 500 K [3,6,11,41,42]. Therefore, to study the influence of surface roughness on these parameters, we used contact layers of nickel obtained by ion-plasma sputtering.

Before loading into the chamber of sputtering system, the second stage of surface preparation of TE material was carried out, which were washed in isopropyl alcohol followed by drying with nitrogen. The contacts were formed using a high-vacuum deposition system Angstrom EvoVac 34. Vacuum-thermal annealing of samples was carried out directly in the chamber at an initial pressure of  $7 \cdot 10^{-8}$  Torr and a temperature of 473 K. After annealing, the surface of the samples was cleaned by bombardment with argon ions for 30 seconds. In the process of vacuum thermal annealing, the quality of the final cleaning of the surface of the samples was controlled using the SRS RGA 200 quadrupole, which is part of the deposition system.

Ion-plasma sputtering of nickel contacts was carried out after ionic cleaning and reaching the working pressure in the chamber. Sputtering modes are as follows: pressure in the chamber —  $7 \cdot 10^{-8}$  Torr; deposition rate — 2 Å/s; gas pressure (Ar) —  $2 \cdot 10^{-3}$  Torr. Ni was deposited onto an unheated surface of TE material. Ni deposition was carried out on samples with different surface roughness. The thickness of the deposited layers was 200, 300, and 400 nm,

with a spread in thickness for each batch of samples not exceeding 5%.

#### 3.2. Research methods

In this work, the determination of the surface roughness of samples after mechanical treatment was carried out using a KLA-Tencor P-7 profilometer. The same device was used to determine the thickness of the deposited Ni layers, with an error not exceeding 5%. For this purpose, a step was formed on a nickel film using photolithography.

The adhesive strength of the films deposited onto the samples was measured by the method of uniform normal tear using a Force Gauge PCE-FM50 device. To optimize the measurement process, nickel contact pads were formed using photolithography with an area of 1 mm<sup>2</sup>. After that, measuring consoles made of nickel wire 0.5 mm in diameter and 30 mm in height were installed on the contact pads using soldering. The console had a clamp for gripping it with the measuring rod of the installation. The adhesion strength was measured in terms of the tear force per unit area (Pa). The specified technique allows measurements with an error not exceeding 10%.

The contact resistance was determined by a four-wire circuit using a technique developed by the authors. The technique is based on the measurement of the total electrical resistance, which consists of the transient contact resistance and the resistance of TE material, with its subsequent exclusion. For this purpose, contact pads were formed by the same way as for measuring adhesion. The distance between the pads was 2 mm. Current and potential wires were soldered to the pads. A current, with a value of 100 mA, was passed in series to the contact pads using current wires. To eliminate the influence of thermoelectric effects, voltage measurements were carried out in opposite directions of the current. The voltage drop was measured using potential wires between the first and subsequent pads.

To study the surface morphology of samples, a JEOL JSM 6010 PLUS/LA scanning electron microscope was used. The study of the samples was carried out in vacuum at a pressure in the working chamber of  $7.5 \cdot 10^{-7}$  Torr. The images were obtained at an accelerating voltage of 20 kV using a secondary electron detector. During the studies, the samples of TE material were positioned at an inclination of 30° with respect to the primary electron beam.

To study the boundary region of the TE material-Ni contact, we used a PHI-670xi raster Auger electron spectrometer from Physical Electronics with a field emission Schottky thermocathode. Auger spectra were recorded at an accelerating voltage of the primary electron beam of 5 kV, primary current  $I_p = 18$  nA. A sample of TE material with a deposited nickel contact was inclined 30° from the normal position to the primary beam. This is necessary for the possibility of ionic cleaning of the surface with an Ar<sup>+</sup> beam and profile analysis. The sample surface was sputtered with Ar<sup>+</sup> ions at an accelerating voltage of 2 kV and a current of 0.5 μA at an angle of 30°. Auger signals were recorded

**Table 1.** Results of calculating the free energy of reactions at different temperatures

Chemical reaction	$\Delta G_{300}$ kJ/mol	$\Delta G_{400}$ kJ/mol	$\Delta G_{500}$ kJ/mol	$K_T$ (300 K)
$3\text{Ni} + 2\text{Bi}_2\text{Te}_3 = 3\text{NiTe}_2 + 4\text{Bi}$	108.15	108.30	108.31	$1.44^{-19}$
$3\text{Ni} + \text{Bi}_2\text{Te}_3 = 3\text{NiTe} + 2\text{Bi}$	-120.76	-133.49	-147.92	$1.08^{21}$
$5\text{Ni} + \text{Sb}_2\text{Te}_3 = 2\text{NiSb} + 3\text{NiTe}$	-270.81	-289.86	-313.80	$1.50^{47}$
$3\text{Ni} + \text{Sb}_2\text{Te}_3 = 3\text{NiTe} + 2\text{Sb}$	-62.43	-70.65	-82.64	$7.5 \cdot 10^{10}$

in a region with a diameter of about  $30\mu\text{m}$  to eliminate the unevenness of Auger emission due to the roughness of the surface of the samples of TE material.

#### 4. Results and discussion

When analyzing the factors influencing the adhesion strength, the following assumptions were made. Internal stresses in the studied films with a thickness of 200, 300, and 400 nm, obtained under the same conditions, have similar values. The values of these stresses at the indicated thicknesses are insignificant. The same applies to the factors  $F_g$  and  $F_e$  (1). Thus, the adhesion strength for the formed nickel contacts will be largely determined by the factors  $F_a$  and  $F_n$ .

To assess the equilibrium adhesion ( $F_a$ ), the thermodynamically most probable reactions of the interaction of nickel with elements of TE material were calculated. As a result of calculating the free energy of reactions, taking into account the data of [43,44], the reactions that can occur when nickel is deposited on TE material were established (Table 1).

The Gibbs free energy of reactions was calculated in the second Ulich approximation, i.e.  $\Delta C_p \neq f(T)$ , according to the formula:

$$\Delta G_T = \Delta H_{298}^0 + \Delta C_p(T - 298) - T\Delta S_{298}^0 - T\Delta C_p \ln(T/298), \quad (2)$$

where  $\Delta G_T$  is Gibbs free energy,  $\Delta H_{298}^0$  is the enthalpy of formation,  $\Delta S_{298}^0$  is standard entropy,  $\Delta C_p$  is change in the isobaric specific heat of the reaction,  $T$  is temperature.

Table 1 also shows the equilibrium constant  $K_T$ , which determines the ratio of the concentration of the reaction products to the concentration of the starting substances:

$$K_T = \exp(-\Delta G_T/RT), \quad (3)$$

where  $R$  — universal gas constant.

Based on the calculation results, the formation of nickel ditelluride is thermodynamically impossible, even with a significant increase in temperature. The formation of monotellurides and antimonides is most probable. The equilibrium constant shows that the interaction of nickel with TE material occurs almost completely and is limited by extremely low mutual diffusion at low temperatures.

The formation of chemical bonds between nickel and TE material at the initial stage of film formation contributes to an increase in adhesion. However, this layer should have a small thickness. At elevated temperatures, both the mutual diffusion of nickel and elements of TE material and the probability of an endothermic reaction increase. This enhances the interaction of nickel with elements of TE material and, as a consequence, the thickness of the transition layer increases. The formation of a layer of intermetallic compounds of considerable thickness in the contact area at elevated temperatures leads to a decrease in the mechanical strength and an increase in the electrical resistance of the contact. This phenomenon was observed

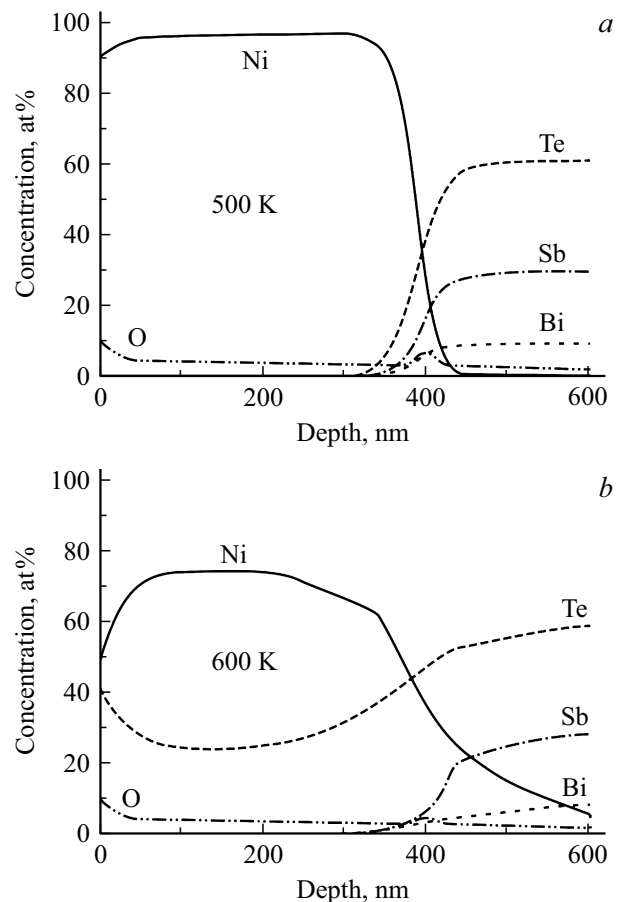


**Figure 1.** Auger depth profiles of the distribution of elements in the structure of the Ni–TE material contact at temperatures of 500 and 600 K.

**Table 2.** Results of the study of Ni films

Ni film thickness, nm	Sample surface roughness, nm	$F$ , MPa	Contact resistance, $\Omega \cdot m^2$
200	70	9.0	$0.9 \cdot 10^{-9}$
	90	10.2	$0.9 \cdot 10^{-9}$
	150	12.6	$0.9 \cdot 10^{-9}$
	225	10.5	$2.2 \cdot 10^{-9}$
	340	8.5	$4.9 \cdot 10^{-9}$
300	70	8.3	$0.8 \cdot 10^{-9}$
	95	9.8	$0.9 \cdot 10^{-9}$
	140	11.9	$1.0 \cdot 10^{-9}$
	200	13.4	$0.9 \cdot 10^{-9}$
	350	10.2	$2.2 \cdot 10^{-9}$
	500	7.8	$8.9 \cdot 10^{-9}$
400	90	9.3	$0.9 \cdot 10^{-9}$
	150	11.7	$1.0 \cdot 10^{-9}$
	280	14.9	$0.9 \cdot 10^{-9}$
	420	11.9	$2.8 \cdot 10^{-9}$
	720	5.5	$9.2 \cdot 10^{-9}$

by a number of authors [6,11,41,45]. In this regard, it is not recommended to use, for example, nickel contacts in thermoelements at temperatures above 500 K.

The possibility of the formation of a transition layer of Ni compounds in the contact region and its increase with temperature are confirmed experimentally by the data of Auger spectroscopy of films with a thickness of 400 nm formed on TE material (Fig. 1). At temperatures up to 500 K, insignificant mutual diffusion of Ni, Te, Sb and Bi is observed in the contact area. As a result of annealing of samples of TE material with nickel contacts at a temperature of 600 K for 60 min, intense mutual diffusion of elements occurs with a significant increase in the transition layer (Fig. 1). It is possible to eliminate the diffusion process at elevated temperatures by forming contact systems with a barrier layer on thermoelements, for example, from molybdenum (Mo/Ni) [6].

Thus, the obtained results suggest that nickel compounds with elements of TE material are formed at the contact interface. The resulting chemical bond determines the equilibrium adhesion values.  $F_a$  can be estimated from adhesive strength measurements. This value mainly determines  $F$  with a low surface roughness of TE material.

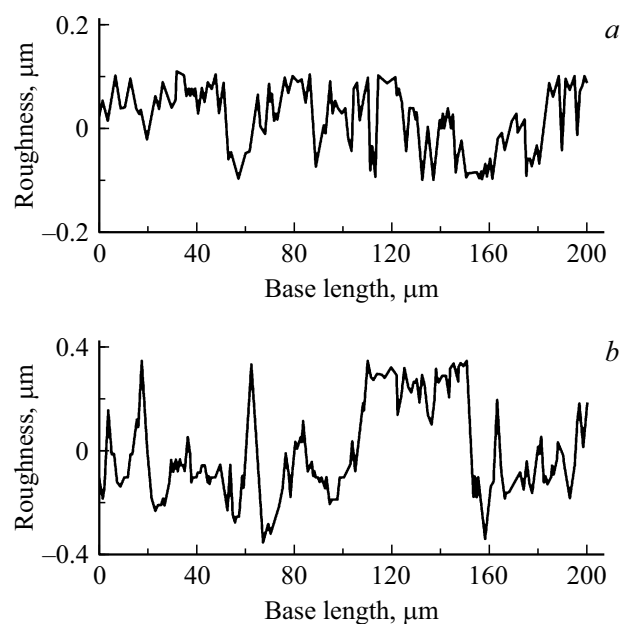
The adhesion strength is largely influenced by the roughness of the substrate surface, which increases the area of actual contact between the film and the substrate and is determined by the value of  $F_n$  in the adhesion strength equation (1). To assess the influence of roughness on adhesion strength, 3 batches of 5–6 samples with surface roughness were made: 70–340 nm for deposition of films with a thickness of 200 nm; 70–500 nm for films with a thickness of 300 nm; 90–720 nm for films with a thickness of 400 nm.

The results of studying the surface relief of TE material with maximum roughness up to 100 nm and 350 nm within the base measurement length (200  $\mu m$ ) are shown in Fig. 2.

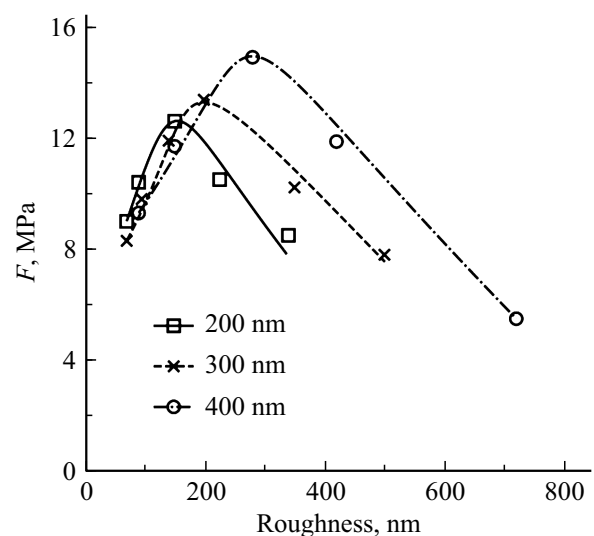
The results of measuring the adhesion strength of nickel films deposited on TE material with different surface roughness are presented in Table 2.

Figure 3 shows the dependences of the adhesion strength of nickel films with a thickness of 200, 300, and 400 nm on the roughness of the surface of TE material.

Based on the research results, the following conclusion can be drawn. At low roughness, the values of the adhesion strength, determined mainly by the factor  $F_a$ , for Ni films of various thicknesses have similar values. The difference



**Figure 2.** Typical surface relief of TE material with roughness of 100 nm (a) and 350 nm (b).



**Figure 3.** Dependences of the adhesion strength of Ni films of various thicknesses on the surface roughness of TE material.

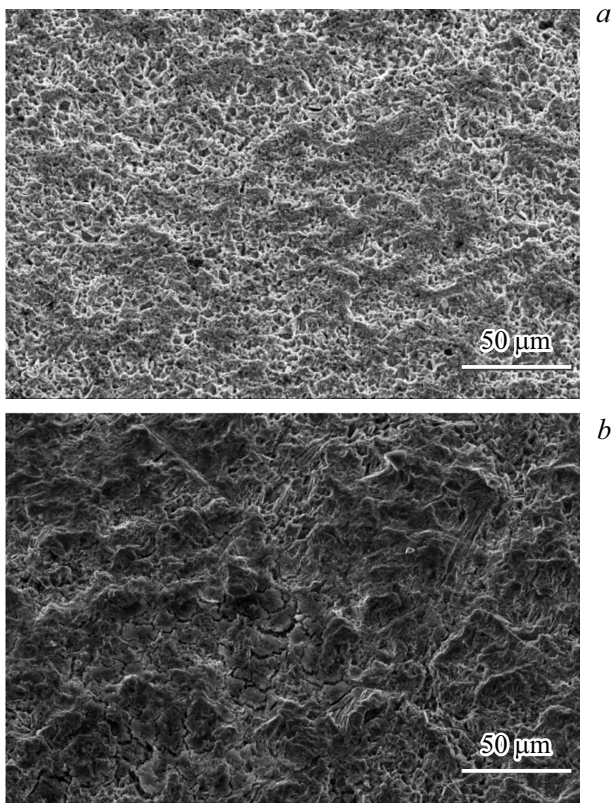


**Figure 4.** Morphology of a Ni film formed on samples of TE material with surface roughness of 200 (a) and 500 nm (b).

in values is at the level of measurement error. With an increase in roughness and, accordingly, the area of actual contact between the film and TE material, the adhesion strength increases. The maximum  $F$  for films 200 nm thick is 12.6 MPa at a roughness of about 150 nm. For films with a thickness of 300 nm, the maximum adhesive strength is 13.4 MPa at a roughness of 220 nm. Films with a thickness of 400 nm have a maximum adhesive strength of 14.9 MPa at a roughness of 280 nm. The maximum values of adhesion strength are observed for a surface roughness corresponding to 70–75% of the film thickness. With a further increase in the surface roughness of the TE material, the adhesive strength decreases. When comparing the adhesion of films of different thicknesses, it should be noted that the maximum values of  $F$  are observed for films with a greater thickness and, accordingly, a greater surface roughness. This statement will be valid at close film thicknesses. It should be noted that with an increase in the film thickness, the role of the internal stress factor increases, which reduces the adhesive strength.

The decrease in adhesion strength with an increase in the surface roughness of TE material is explained as follows. High roughness with sharp peaks and valleys leads to deformation of the film. If the surface roughness of the TE material is comparable with the thickness of the film, its breaks are possible and, as a consequence, a decrease

in adhesion and an increase in the electrical resistance of contacts. Violation of the integrity of the film is observed in the images of its surface obtained using scanning electron microscope. Figure 4 shows the morphology of 300 nm thick nickel films formed on samples of TE material with surface roughness of 200 and 500 nm. At a roughness of 200 nm, a uniform Ni layer is observed. At a roughness of 500 nm, defects are noticeable on the surface of the Ni film.

With increased roughness, in addition to a decrease in adhesion strength, there is an increase in contact resistance (Table 2), which is also associated with defects in the Ni film. We observed similar phenomena during the formation of contact systems to thermoelements made from various TE materials [6].

The results of the studies carried out made it possible to optimize the technological process of obtaining contact systems for thermoelements with high adhesive strength and low contact resistance.

## 5. Conclusions

Thermoelements operate at high temperature gradients, and generator thermoelements in a wide temperature range, often under conditions of increased vibration. Moreover, the construction of the thermoelement uses materials with different thermal expansion coefficients. All this leads to high mechanical loads in the thermoelement structure, which are limited by the adhesive strength of the contacts.

The analysis of factors influencing the adhesive strength of film coatings was carried out. Investigations of the influence of these factors on the adhesive strength of thin-film nickel contacts obtained by ion-plasma sputtering on samples of TE material were carried out. It was found that the formation of a layer of limited dimensions in the near-boundary region of nickel compounds with elements of TE material increases the equilibrium adhesion. It was shown that the formation of nickel monotellurides and antimonides is possible at the boundary. With the help of Auger electron spectroscopy, it was established that nickel contacts are thermally stable at temperatures not exceeding 500 K. The influence of the surface roughness of the TE material on the adhesion strength of contacts was investigated. It was found that, on the one hand, the roughness increases the area of actual contact between the film and TE material, and, accordingly, its adhesion strength. On the other hand, high roughness with sharp peaks and valleys leads to deformation of the film. It is shown that with a roughness comparable to and greater than the thickness of the film, its ruptures are possible and, as a consequence, a decrease in adhesion and an increase in the electrical resistance of contacts. The optimal ratio of the film thickness and the roughness of the surface of TE material, at which the maximum adhesion is observed, was determined. This roughness is 70–75% of the deposited film thickness.

The studies of the electrical resistivity of the contacts were carried out; an increase in this parameter at a high

roughness was shown. The methods of surface preparation of TE material and modes of ion-plasma sputtering have been optimized. This made it possible to obtain thermostable contacts to thermoelements with low resistivity, of the order of  $10^{-9} \Omega \cdot \text{m}^2$  and high adhesive strength of at least 12 MPa.

## Funding

This work was supported by the Russian Science Foundation (grant number 21-19-00312).

## Conflict of interest

The authors declare that they have no conflict of interest.

## References

- [1] W. Liu, S. Bai. *J. Materiomics*, **5**, 321 (2019).
- [2] H.J. Goldsmid. *Introduction to Thermoelectricity* (Berlin, Springer, 2016).
- [3] X. Zhu, L. Cao, W. Zhu, Y. Deng. *Adv. Mater. Interfaces*, **5**, 1801279 (2018).
- [4] L.M. Vikhor, L.I. Anatychuk, P.V. Gorskyi. *J. Appl. Phys.*, **126**, 164503 (2019).
- [5] G. Joshi, D. Mitchell, J. Ruedin, K. Hoover, R. Guzman, M. McAleer, L. Wood, S. Savoy. *J. Mater. Chem. C*, **7**, 479 (2019).
- [6] M. Shtern, M. Rogachev, Y. Shtern, D. Gromov, A. Kozlov, I. Karavaev. *J. Alloys Compd.*, **852**, 156889 (2021).
- [7] S. Twaha, J. Zhu, Y. Yan, B. Li. *Renew. Sust. Energ. Rev.*, **65**, 698 (2016).
- [8] C.L. Cramer, H. Wang, K. Ma. *J. Electron. Mater.*, **47**, 5122 (2018).
- [9] P.H. Ngan, L. Han, D.V. Christensen. *J. Electron. Mater.*, **47**, 701 (2018).
- [10] L. Cai, P. Li, Q. Luo, P. Zhai, Q. Zhang. *J. Electron. Mater.*, **46**, 1552 (2017).
- [11] D.G. Gromov, Yu.I. Shtern, M.S. Rogachev, A.S. Shulyat'ev, E.P. Kirilenko, M.Yu. Shtern, V.A. Fedorov, M.S. Mikhailova. *Inorg. Mater.*, **52** (11), 1132 (2016).
- [12] M. Shtern, M. Rogachev, Y. Shtern, A. Kozlov, A. Sherchenkov, E. Korchagin. In: *Proc. 2021 International Seminar on Electron Devices Design and Production* (Prague, Czech Republic, 2021) p. 9444502.
- [13] J. Chu, J. Huang, R. Liu, J. Liao, X. Xia, Q. Zhang, C. Wang, M. Gu, S. Bai, X. Shi, L. Chen. *Nature Communications*, **11**, 2723 (2020).
- [14] L.-W. Chen, C. Wang, Y.-C. Liao, C.-L. Li, T.-H. Chuang, C.-H. Hsueh. *J. Alloys Compd.*, **762**, 631 (2018).
- [15] D. Qin, W. Zhu, F. Hai, C. Wang, J. Cui, Y. Deng. *Adv. Mater. Interfaces*, **6** (20), 1900682 (2019).
- [16] P.A. Sharma, M. Brumbach, D.P. Adams, J.F. Ihlefeld, A.L. Lima-Sharma, S. Chou, J.D. Sugar, P. Lu, J.R. Michael, D. Ingersoll. *AIP Adv.*, **9** (1), 015125 (2019).
- [17] R.P. Gupta, J.B. White, O.D. Iyore, U. Chakrabarti, H.N. Alshareef, B.E. Gnade. *Electrochem. Solid-State Lett.*, **12** (8), H302 (2009).
- [18] P.J. Taylor, J.R. Maddux, G. Meissner, R. Venkatasubramanian, G. Bulman, J. Pierce, R. Gupta, J. Bierschenk, C. Caylor, J. D'Angelo. *Appl. Phys. Lett.*, **103** (4), 043902 (2013).
- [19] S.-P. Feng, Y.-H. Chang, J. Yang, B. Poudel, B. Yu, Z. Ren, G. Chen. *Phys. Chem. Chem. Phys.*, **15** (18), 6757 (2013).
- [20] B.V. Deryagin, N.A. Krotova, V.P. Smilga. *Adhesion of solids* (M., Nauka, 1973) [in Russian].
- [21] M.Yu. Shtern, I.S. Karavaev, Y.I. Shtern, A.O. Kozlov, M.S. Rogachev. *Semiconductors*, **53** (13), 1848 (2019).
- [22] A.D. Zimon. *Adhesion of films and coatings* (M., Himiya, 1977) [in Russian].
- [23] S. Morrison. *The Chemical Physics of Surfaces* (N.Y., Springer US, 1977).
- [24] T. Sakamoto, Y. Taguchi, T. Kutsuwa, K. Ichimi, S. Kasatani, M. Inada. *J. Electron. Mater.*, **45**, 1321 (2016).
- [25] G. Joshi, D. Mitchell, J. Ruedin, K. Hoover, R. Guzman, M. McAleer, L. Wood, S. Savoy. *J. Mater. Chem. C*, **7**, 479 (2019).
- [26] S. Kashi, M.K. Keshavarz, D. Vasilevskiy, R.A. Masut, S. Turenne. *J. Electron. Mater.*, **41**, 1227 (2012).
- [27] S.M. Sze, K.K. Ng. *Physics of Semiconductor Devices* (N.Y., Wiley, 2007).
- [28] *Thick and thin films for electronic applications*, ed. by A. Reisman, K. Rose (N.Y., Wiley, 1971)
- [29] E.H. Rhoderick, R.H. Williams. *Metal-Semiconductor Contacts* (Oxford, University Press, 1988).
- [30] C.H. Wang, H.C. Hsieh, H.Y. Lee, A.T. Wu. *J. Electron. Mater.*, **48**, 53 (2019).
- [31] J. Cheng, X. Hu, Q. Li. *J. Mater. Sci. Mater. Electron.*, **31**, 14714 (2020).
- [32] Y.N. Nguyen, S. Kim, S.H. Bae, I. Son. *Appl. Surf. Sci.*, **545**, 149005 (2021).
- [33] X.A. Fan, J.Y. Yang, R.G. Chen, H.S. Yun, W. Zhu, S.Q. Bao, X.K. Duan. *J. Phys. D Appl. Phys.*, **39**, 740 (2006).
- [34] S. Duan, N. Man, J. Xu, Q. Wu, G. Liu, X. Tan, H. Shao, K. Guo, X. Yang, J. Jiang. *J. Mater. Chem. A*, **7**, 9241 (2019).
- [35] E. Pozega, S. Ivanov, Z. Stevic, L. Karanovic, R. Tomanec, L. Gomidzelovic, A. Kostov. *Trans. Nonferrous Metals Soc. China*, **25**, 3279 (2015).
- [36] E.Ł. usakowska, S. Adamiak, R. Minikayev, P. Skupinski, A. Szczerbakow, W. Szuszkiewicz. *Acta Phys. Polon. A*, **134**, 941 (2018).
- [37] M.K. Sharov, O.B. Yatsenko, Ya.A. Ugai. *Inorg. Mater.*, **42**, 723 (2006).
- [38] S. Perumal, S. Roychowdhury, K. Biswas. *Inorg. Chem. Front.*, **3**, 125 (2016).
- [39] M. Samanta, K. Biswas. *J. Am. Chem. Soc.*, **139**, 9382 (2017).
- [40] C.-H. Lee, M.F. Kilicaslan, B. Madavali, S.-J. Hong. *Res. Chem. Intermed.*, **40**, 2543 (2014).
- [41] W. Liu, H. Wang, L. Wang, X. Wang, G. Joshi, G. Chen, Z. Ren. *J. Mater. Chem.*, **1**, 13093 (2013).
- [42] J. de Boor, C. Gloanec, H. Kolb, R. Sottong, P. Ziolkowski, E. Muller. *J. Alloys Compd.*, **632**, 348 (2015).
- [43] *Thermal constants of substances*, ed. by V.P. Glushko (M., VINITI, 1972) [in Russian].
- [44] L.P. Ruzinov, B.S. Gulyackih. *Equilibrium transformations of metallurgical reactions* (M., Metallurgiya, 1975) [in Russian].
- [45] S.W. Chen, T.R. Yang, C.Y. Wu, H.W. Hsiao, H.S. Chu, J.D. Huang, T.W. Liou. *J. Alloys Compd.*, **686**, 847 (2016).